

Emergent Bistability : Effects of Additive and Multiplicative Noise

Sayantari Ghosh, Subhasis Banerjee, and Indrani Bose*

Department of Physics, Bose Institute, 93/1 Acharya Prafulla Chandra Road, Kolkata - 700009, India

Positive feedback and cooperativity in the regulation of gene expression are generally considered to be necessary for obtaining bistable expression states. Recently, a novel mechanism of bistability termed emergent bistability has been proposed which involves only positive feedback and no cooperativity in the regulation. An additional positive feedback loop is effectively generated due to the inhibition of cellular growth by the synthesized proteins. The mechanism, demonstrated for a synthetic circuit, may be prevalent in natural systems also as some recent experimental results appear to suggest. In this paper, we study the effects of additive and multiplicative noise on the dynamics governing emergent bistability. The calculational scheme employed is based on the Langevin and Fokker-Planck formalisms. The steady state probability distributions of protein levels and the mean first passage times are computed for different noise strengths and system parameters. In the region of bistability, the bimodal probability distribution is shown to be a linear combination of a lognormal and a Gaussian distribution. The variances of the individual distributions and the relative weights of the distributions are further calculated for varying noise strengths and system parameters. The experimental relevance of the model results is also pointed out.

* indrani@bosemain.boseinst.ac.in

I. INTRODUCTION

Gene expression, a fundamental activity in the living cell, is a complex sequence of events resulting in protein synthesis [1]. In the case of deterministic time evolution, the temporal rate of change of protein concentration is given by the difference between the rates of synthesis and decay of proteins. When these rates balance each other the net rate of change is zero and one obtains a steady state described by a fixed protein concentration. In the case of positively regulated gene expression, the dynamics may result in bistability, i.e., the existence of two stable steady states for the same parameter values [2–4]. Bistability, in general, is an outcome of dynamics involving positive feedback and sufficient nonlinearity. One way of achieving the latter condition is when multiple bindings of regulatory molecules occur at the promoter region of the gene (cooperativity in regulation) or when the regulatory proteins form multimers like dimers and tetramers which then bind the specific regions of the DNA [2–5]. The simplest example of bistability in gene expression is that of a gene the protein product of which promotes its own synthesis [5, 6]. Positive autoregulation occurs via the binding of protein dimers at the promoter region resulting in the activation of gene expression. Experimental evidence of bistability has been obtained in a wide range of biological systems, e. g. , the lysis-lysogeny genetic circuit in bacteriophage λ [7], the lactose utilization network in *E. coli* [8], the network of coupled positive feedback loops governing the transition to the mitotic phase of the eukaryotic cell cycle [9], the development of competence in the soil bacteria *B. subtilis* [4, 10] and more recently the activation of the stringent response in mycobacteria subjected to nutrient depletion [11, 12]. A number of synthetic circuits have also been constructed which exhibit bistable gene expression under appropriate conditions [13–15].

Recently, Tan et al. [16] have proposed a new mechanism by which bistability arises, termed emergent bistability, in which a noncooperative positive feedback circuit combined with circuit induced growth retardation of the embedding cell give rise to two stable expression states. The novel type of bistability was demonstrated in a synthetic gene circuit consisting of a single positive feedback loop in which the protein product X of a gene promotes its own synthesis in a noncooperative manner. If the circuit is considered in isolation, one obtains monostability, i.e., a single stable steady state. In the actual system, the production of protein X has a retarding effect on the growth of the host cell so that the circuit function is linked to cellular growth. The protein decay rate has, in general, two components, the natural degradation rate and the dilution rate due to cell growth. Since the latter is reduced on increased protein production, a second positive feedback loop is effectively generated, as illustrated in Fig. 1. An increased synthesis of protein X leads to a lower dilution rate, i.e., a greater accumulation of the protein which in turn promotes a higher amount of protein production. Tan et al. [16] developed a mathematical model to capture the essential dynamics of the system of two positive feedback loops and showed that in a region of parameter space bistable gene expression is possible. The rate equation governing the dynamics of the system is given by [16]

$$\frac{dx}{dt} = \frac{\delta + \alpha x}{1 + x} - \frac{\phi x}{1 + \gamma x} - x \quad (1)$$

where the variables and the parameters are nondimensionalized with x being a measure of the protein amount. The parameter δ is the rate constant associated with basal gene expression, α represents the effective rate constant for protein synthesis, ϕ denotes the maximum dilution rate due to cell growth and γ is a parameter denoting the ‘metabolic burden’. When limited resources are available to the cell, the synthesis of proteins imposes a metabolic cost, i.e., the availability of resources for cellular growth is reduced. The form of the nonlinear decay rate (the second term in Eq. (1)) is arrived at using the Monod model [17] which takes into account the effect of resource or nutrient limitation on the growth of a cell population. An alternative explanation for the origin of the nonlinear protein decay rate is based on the fact that the synthesis of a protein may retard cell growth if it is toxic to the cell [18].

The experimental signature of bistability lies in the coexistence of two subpopulations with low and high protein levels. In the case of deterministic dynamics, the cellular choice between two stable expression states is dictated by the previous history of the system [2–4, 14]. In this picture, if the cells in a population are in the same initial state, the steady state should be the same in each cell. The experimental observation of population heterogeneity in the form of two distinct subpopulations can be explained once the stochastic nature of gene expression [19, 20] is taken into account. Bistable gene expression is characterized by the existence of two stable steady states separated by an unstable steady state. A transition from the low to the high expression state, say, is brought about once the fluctuations associated with the low expression level cross the threshold set by the protein concentration in the unstable steady state [6, 10, 21]. Noise-induced transitions between the stable expression states give rise to a bimodal distribution in the protein levels. In a landscape picture, the two stable expression states correspond to the two minima of an expression potential and the unstable steady state is associated with the top of the barrier separating the two valleys [22]. A number of examples is now known which illustrate the operation of stochastic genetic switches between well-defined expression states [7, 10–12, 23–26]. Stochasticity in gene expression has different possible origins, both intrinsic and extrinsic. The biochemical events (reactions) involved in gene expression are probabilistic in nature giving rise to fluctuations (noise) around mean mRNA and protein levels. The randomness in the timing of a reaction arises from the fact that the reactants have

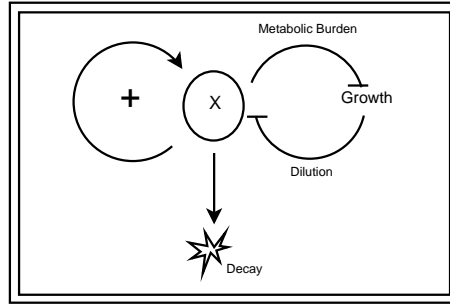


Figure 1. A genetic circuit illustrating emergent bistability. The protein product X of a gene promotes its own synthesis as well as retards the growth of the host cell. Growth retardation combined with a lower dilution rate of the protein concentration effectively generate a second positive feedback loop. The arrowhead in a regulatory link denotes activation and the hammerhead symbol denotes repression.

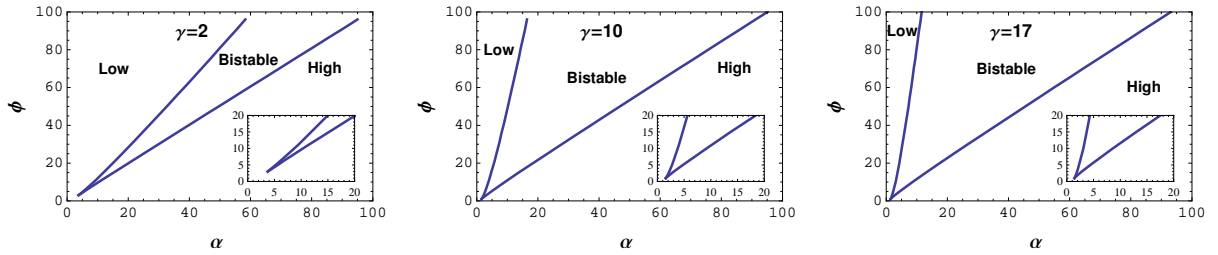


Figure 2. Bifurcation diagrams corresponding to Eq. (1) in the $\phi - \alpha$ plane with $\gamma = 2, 10$ and 17 in the successive plots. (inset) Portions of bifurcation diagrams amplified to indicate how a transition from the low to the high expression state can be brought about without passing through the region of bistability. The rate constant $\delta = 0.01$.

to collide with each other and the energy barrier separating the reactants from the product state has to be crossed for the occurrence of the reaction. The stochastic time evolution of the system can be studied using the Master Equation (ME) approach [27, 28]. The ME is a differential equation describing the temporal rate of change of the probability that the system is in a specific state at time t . The state at time t is described in terms of the number of biomolecules (mRNAs, proteins etc.) present in the system at t . The solution of the ME gives a knowledge of the probability distribution the lower two moments of which yield the mean and the variance. One is often interested in the steady state solution of the ME, i.e., when the temporal rate of change of the probability is zero. The ME has exact, analytical solutions only in the cases of simple biochemical kinetics. A rigorous simulation technique based on the Gillespie algorithm [29] provides a numerical solution of the ME. The computational cost in terms of time and computer memory can, however, become prohibitive as the complexity of the system studied increases. Two approximate methods for the study of stochastic processes are based on the Langevin and Fokker-Planck (FP) equations [27, 28]. These equations are strictly valid in the case of large numbers of molecules so that a continuous approximation is justified and the system state is defined in terms of concentrations of molecules rather than numbers. In fact, both the equations are obtained from the ME in the large molecular number limit. In the Langevin equation (LE) additive and multiplicative stochastic terms are added to the rate equation governing the deterministic dynamics. The corresponding FP equation is a rate equation for the probability distribution [27, 28]. Noise in the form of random fluctuations has a non-trivial effect on the gene expression dynamics involving positive feedback [22, 30–32]. In this paper, we investigate the effects of additive and multiplicative noise on the dynamics, described by Eq. (1), with special focus on emergent bistability. In Sec. II, we first present the bifurcation analysis of Eq. (1) and then describe the general forms of the Langevin and FP equations as well as the expression for the steady state probability distribution of the protein levels in an ensemble of cells. Sec. III contains the results of our study when only additive as well as when both additive and multiplicative types of noise are present. In Sec. IV, the mean first passage times for escape over the potential barrier are computed. In Sec. V, we discuss the significance of the results obtained and also make some concluding remarks.

II. LANGEVIN AND FOKKER-PLANCK EQUATIONS

In Eq. (1), the steady state condition $\frac{dx}{dt} = 0$ results in bistability, i.e., two stable gene expression states in specific parameter regions. Fig. 2 represents the bifurcation diagrams in the $\phi - \alpha$ plane for different values of the metabolic cost parameter γ . The region of bistability is bounded by lines at which bifurcation from bistability to monostability occurs. The steady states in the region of bistability are the three physical solutions (x real and positive) of the cubic polynomial equation obtained from Eq. (1) by putting $\frac{dx}{dt} = 0$. Two of the

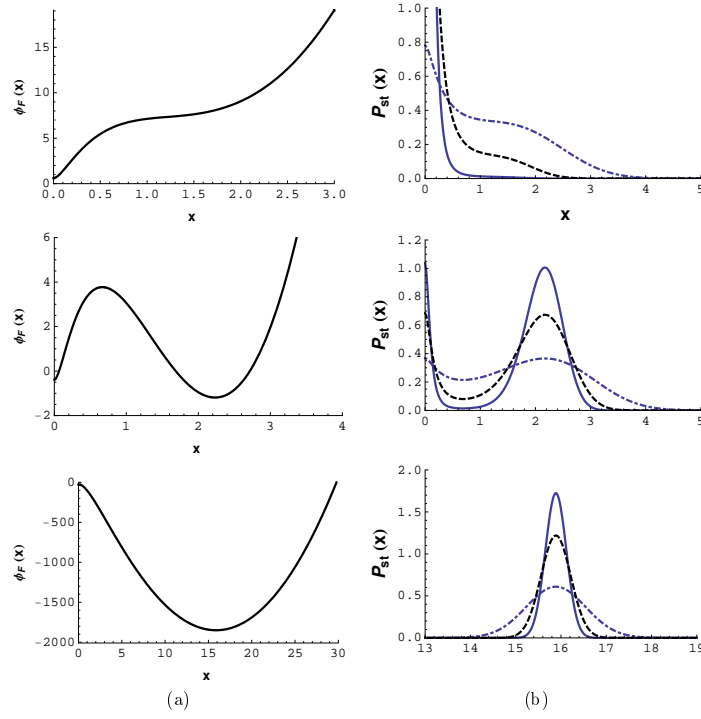


Figure 3. **(a)** Stochastic potential $\phi_F(x)$ (Eq. (16)) in the case of purely additive noise as the parameter α is tuned from low to high values ($\alpha = 5.5, 5.96$ and 19). The other parameter values are $\gamma = 10$, $\delta = 0.01$, and $\phi = 20$ with the noise strength kept fixed at $D_2 = 0.05$. **(b)** Steady state probability distribution, $P_{st}(x)$, for successive values of $\alpha = 5.5, 5.96$ and 19 . For each values of α , $P_{st}(x)$ is computed and displayed for three different noise strengths $D_2 = 0.05$ (solid line), $D_2 = 0.1$ (dashed line), $D_2 = 0.4$ (dot-dashed line).

solutions correspond to stable steady states and these are separated by an unstable steady state represented by the third solution. At the bifurcation point separating bistability from the monostable low expression state, the higher stable state solution merges with the unstable steady state solution. Similarly, at the bifurcation point separating bistability from the monostable high expression state, the lower two solutions merge so that away from this point and towards the right in the $\phi - \alpha$ plane only the stable high expression state survives. The bifurcation analysis has been carried out using the software package Mathematica. One notes that the extent of the region of bistability increases as the value of the parameter γ increases. When $\gamma = 0$, i.e., the net decay rate of the proteins has the form $-(\phi + 1)x$, there is no region of bistability in the parameter space. For $\gamma \neq 0$, one can pass from a monostable low expression state across a region of bistability to a monostable high expression state by increasing α and decreasing ϕ . One also observes that one can directly go from the low to the high expression state without passing through the region of bistability. The region of parameter space through which the bypass can occur is dependent on γ , diminishing in size with increasing values of γ . We next include appropriate noise terms in Eq. (1) to investigate the effects of noise on the deterministic dynamics.

The general stochastic formalism based on the Langevin and FP equations for the steady state analysis of a bistable system is described in Refs. [27, 28, 33, 35–37]. We apply the formalism to investigate the effects of additive and multiplicative noise on emergent bistability, the governing equation of which is described in Eq. (1). We consider an one-variable LE containing a multiplicative and an additive noise term:

$$\frac{dx}{dt} = f(x) + g_1(x)\epsilon(t) + \Gamma(t) \quad (2)$$

where $\epsilon(t)$ and $\Gamma(t)$ represent Gaussian white noises with mean zero and correlations given by

$$\begin{aligned} \langle \epsilon(t)\epsilon(t') \rangle &= 2D_1\delta(t-t') \\ \langle \Gamma(t)\Gamma(t') \rangle &= 2D_2\delta(t-t') \\ \langle \epsilon(t)\Gamma(t') \rangle &= \langle \Gamma(t)\epsilon(t') \rangle = 2\lambda\sqrt{D_1D_2}\delta(t-t') \end{aligned} \quad (3)$$

D_1 and D_2 are the strengths of the two types of noise $\epsilon(t)$ and $\Gamma(t)$ respectively and λ is the degree of correlation between them. The first term, $f(x)$, in Eq. (2) represents the deterministic dynamics. With the dynamics governed by Eq. (1), the function $f(x)$ is given by,

$$f(x) = \frac{\delta + \alpha x}{1 + x} - \frac{\phi x}{1 + \gamma x} - x \quad (4)$$

The additive noise $\Gamma(t)$ represents noise arising from an external perturbative influence or originating from some missing information embodied in the rate equation approximation [22]. Gene expression consists of the major steps of transcription and translation which are a complex sequence of biochemical events. Regulation of gene expression as well as processes like cell growth have considerable influence on the gene expression dynamics. In many of the models of gene expression, some of the elementary processes (say, transcription and translation as in the case of the model described by Eq. (1)) are lumped together and an effective rate constant associated with the combined process (e.g., α , the effective rate constant for protein synthesis in Eq. (1)). It is, however, expected that the rate constants fluctuate in time due to a variety of stochastic influences like fluctuations in the number of regulatory molecules and RNA polymerases. In the LE, the fluctuations in the rate constants are taken into account through the inclusion of multiplicative noise terms like $g_1(x)\epsilon(t)$ in Eq. (2). In the present study, we consider two types of multiplicative noise associated with the rate constants α (effective rate constant for protein synthesis) and ϕ (the maximum dilution rate). The rates vary stochastically. i.e., $\alpha \rightarrow \alpha + \epsilon(t)$ with

$$g_1(x) = \frac{x}{1 + x} \quad (5)$$

in one case and $\phi \rightarrow \phi + \epsilon(t)$ with

$$g_1(x) = -\frac{x}{1 + \gamma x} \quad (6)$$

in the other case (see Eq. (1)). As mentioned before, $\epsilon(t)$ represents random fluctuations of the Gaussian white noise-type. There are alternative versions of the LE in which the noise terms added to the deterministic part have an explicit structure in terms of gene expression parameters [7, 29, 34]. Gillespie [29] has shown how to derive the Chemical LE starting with the Master equation describing the stochastic time evolution of a set of elementary reactions with the noise terms depending on the number of molecules as well as the gene expression parameters. Similarly, for an effective kinetic equation of the form

$$\frac{dn}{dt} = f(n) - g(n) \quad (7)$$

where n is the number of molecules and $f(n)$, $g(n)$ the synthesis and decay rates respectively, one can write the LE as [7, 34]

$$\frac{dn}{dt} = f(n) - g(n) + \sqrt{f(n) + g(n)} \Gamma(t) \quad (8)$$

While these alternative approaches have their own merit, the majority of stochastic gene expression studies, based on the Langevin formalism, start with equations of the type shown in (2). The choice is dictated by the simplicity of the calculational scheme with specific focus on the separate effects of additive and multiplicative noise (fluctuating rate constants) on the gene expression dynamics.

The FP equation can be developed from the LE following usual procedure [22, 28, 32]. The FP equation corresponding to Eq. (2) is [22, 28, 32]

$$\frac{\partial P(x, t)}{\partial t} = -\frac{\partial}{\partial x}[A(x)P(x, t)] + \frac{\partial^2}{\partial x^2}[B(x)P(x, t)] \quad (9)$$

where

$$A(x) = f(x) + D_1 g_1(x) g'_1(x) + \lambda \sqrt{D_1 D_2} g'_1(x) \quad (10)$$

and

$$B(x) = D_1 [g_1(x)]^2 + 2\lambda \sqrt{D_1 D_2} g_1(x) + D_2 \quad (11)$$

The steady state probability distribution (SSPD), from Eq. (4), is given by [28, 33, 35]

$$\begin{aligned}
P_{st}(x) &= \frac{N}{B(x)} \exp\left[\int^x \frac{A(x)}{B(x)} dx\right] \\
&= \frac{N}{\{D_1[g_1(x)]^2 + 2\lambda\sqrt{D_1 D_2}g_1(x) + D_2\}^{\frac{1}{2}}} \exp\left[\int^x \frac{f(x')dx'}{D_1[g_1(x')]^2 + 2\lambda\sqrt{D_1 D_2}g_1(x') + D_2}\right]
\end{aligned} \tag{12}$$

where N is the normalization constant. Eq. (12) can be recast in the form

$$P_{st}(x) = N e^{-\phi_F(x)} \tag{13}$$

with

$$\phi_F(x) = \frac{1}{2} \ln[D_1[g_1(x)]^2 + 2\lambda\sqrt{D_1 D_2}g_1(x) + D_2] - \int^x \frac{f(y)dy}{D_1[g_1(y)]^2 + 2\lambda\sqrt{D_1 D_2}g_1(y) + D_2} \tag{14}$$

$\phi_F(x)$ defines the ‘stochastic potential’ corresponding to the FP equation.

III. RESULTS FOR ADDITIVE AND MULTIPLICATIVE NOISE

We first consider the case when only the additive noise term is present in Eq. (2), i.e., the second term on the r.h.s. is missing. The function $f(x)$ is given in Eq. (4). As pointed out in [16], the parameters α (effective rate constant for protein synthesis) and ϕ (maximum dilution rate) are experimentally tunable. From Eqs. (12) and (14), the expression potentials, $\phi_F(x)$, and the associated steady state probability distributions, $P_{st}(x)$, can be computed. The stochastic potential $\phi_F(x)$ has the form

$$\phi_F(x) = \frac{1}{2} \ln D_2 - \frac{1}{D_2} \int^x f(y)dy \tag{15}$$

$$= \frac{1}{2} \ln D_2 + \frac{1}{D_2} \phi_D(x) \tag{16}$$

where $\phi_D(x)$ is the deterministic potential, i.e., $f(x) = -\frac{\partial \phi_D(x)}{\partial x}$. In the presence of only additive noise, the stochastic and deterministic potentials have similar forms. Figure 3 displays $\phi_F(x)$ and $P_{st}(x)$ versus x as the parameter α is tuned from low to high values ($\alpha = 5.5, 5.96, 19$). The other parameter values are kept fixed with $\gamma = 10$, $\delta = 0.01$ and $\phi = 20$, the values being identical to those reported in [16]. For each value of α , the potential $\phi_F(x)$ is plotted only for the noise strength $D_2 = 0.05$ whereas $P_{st}(x)$ is plotted for the noise strengths $D_2 = 0.05$ (solid line), 0.1 (dashed line) and 0.4 (dot-dashed line). One finds that by tuning α from low to high values, one can pass from a monostable low expression state through a region of bistability, i.e., a coexistence of low and high expression states to a monostable high expression state. The region of bistability is distinguished by the appearance of two prominent peaks in the distribution of protein levels. One can also keep α fixed and obtain a similar set of plots by varying the maximum dilution rate ϕ .

The stochastic potential $\phi_F(x)$ is indicative of the steady state stability. In Fig. 3(a), for $\alpha = 5.5$, the potential has a deep (shallow) minimum at low (high) values of x . For low values of the noise strength, e. g. , $D_2 = 0.05$ (solid line), the steady state probability distribution $P_{st}(x)$ has a single prominent peak. Noise can induce transitions from one local minimum to the other of the stochastic potential. The minima represent steady states which are separated by an energy barrier. For $\alpha = 5.5$ and $\alpha = 5.96$, there are two energy barriers corresponding to the transitions from the low to the high expression states and vice versa. In the case of $\alpha = 5.5$, increased magnitudes of the additive noise flip the switch in the unfavorable direction (energy barrier higher) so that $P_{st}(x)$ has a second peak, albeit not prominent, at a higher expression level. When $\alpha = 5.96$, the energy barriers are of similar magnitude and $P_{st}(x)$ has two prominent peaks at low and high expression levels when the noise strength is low ($D_2 = 0.05$). With increased noise strengths, the two expression levels are more readily destabilized resulting in a smearing of the expression levels. $P_{st}(x)$ has now a finite value for intermediate values of x . In the case of $\alpha = 19$, the stochastic potential has a single minimum at the high expression level so that $P_{st}(x)$ is unimodal. With higher values of the noise strength D_2 , the probability distribution becomes broader. One also notes that with increased values of α , the magnitude of the high expression level also increases.

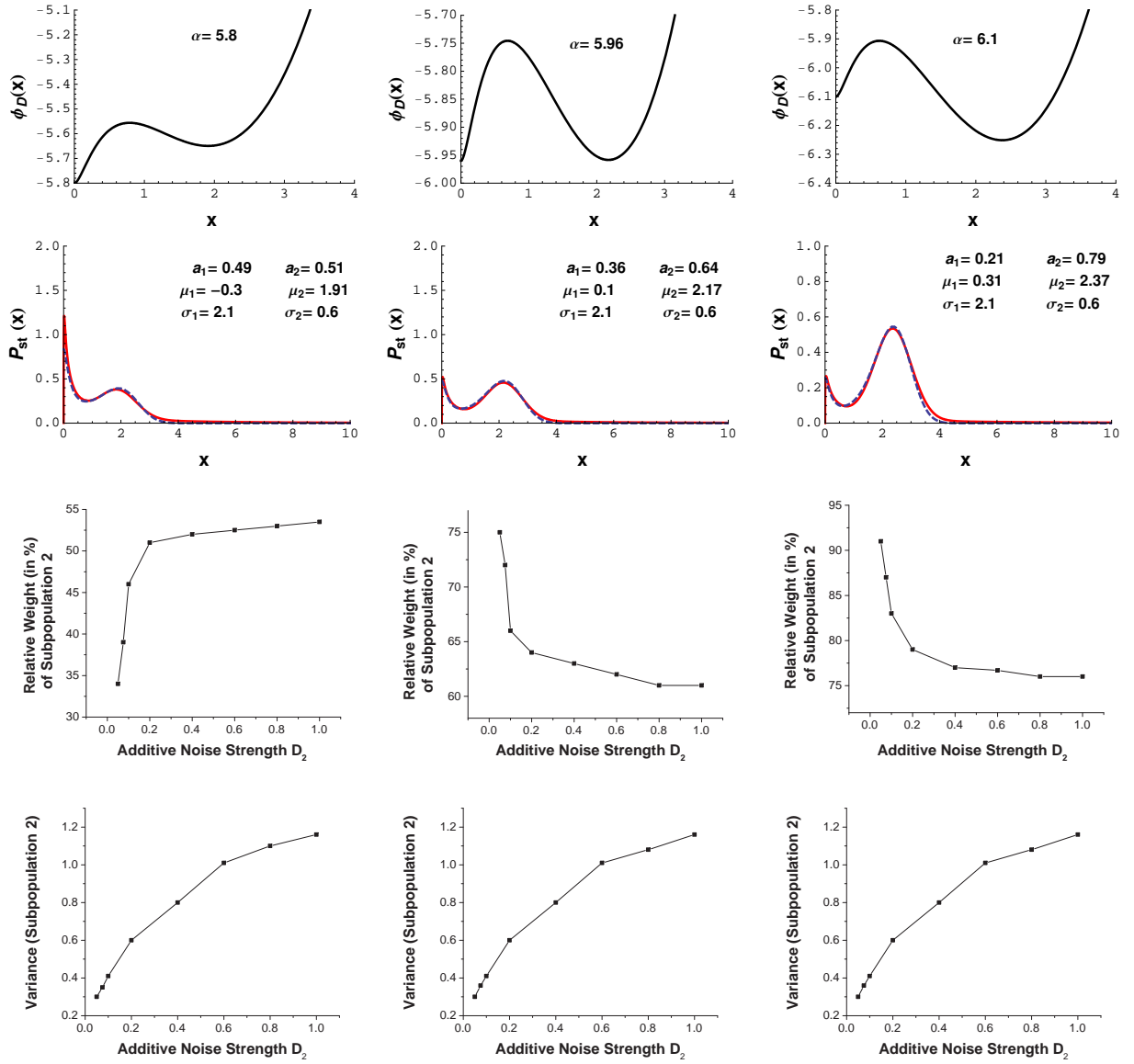


Figure 4. Relative weight of Subpopulation 2 and variance of the associated probability distribution as a function of the additive noise strength D_2 , computed using a mixture model. (First Panel) Deterministic potentials for $\alpha = 5.8, 5.96$ and 6.1 in the region of bistability. The other parameter values are the same as in the case of Fig. 3. (Second Panel) Steady state probability distribution $P_{st}(x)$ versus x (solid line) for $\alpha = 5.8, 5.96$ and 6.1 as fitted by the distribution (dashed line) obtained from a mixture model. The individual probability distributions are lognormal (Subpopulation 1) and Gaussian (Subpopulation 2). The parameters of the distributions and the coefficients a_1 and a_2 are also mentioned ($a_1 + a_2 = 1$). (Third Panel) Relative weight (in percentage) of Subpopulation 2 versus D_2 . (Fourth Panel) Variance of Gaussian probability distribution (Subpopulation 2) as a function of D_2 .

In the region of bistability, the total population is a mixture of two subpopulations. In order to determine the effects of additive noise on the relative weights and variances of the subpopulation probability distributions, we take recourse to a mixture model in which the steady state probability distribution for the total population, $P_{st}(x) = a_1 P_{st1}(x) + a_2 P_{st2}(x)$. $P_{st1}(x)$ and $P_{st2}(x)$ are the steady state probability distributions for Subpopulation 1 and 2 respectively and a_1, a_2 are the coefficients in the linear combination ($a_1 + a_2 = 1$). Subpopulation 1 (2) is characterized by predominantly low (high) expression levels. The upper panel of Fig. 4 shows the deterministic potentials, $\phi_D(x)$, for $\alpha = 5.8, 5.96$ and 6.1 in the region of bistability. The other parameter values are the same as in the case of Fig. 3. The second panel in Fig. 4 shows the steady state probability distributions, $P_{st}(x)$ (solid line), in the three cases as well as the fitting distributions (dashed line) using the mixture model. The additive noise strength D_2 is kept fixed at the value $D_2 = 0.2$. In each case, $P_{st1}(x)$ and $P_{st2}(x)$ are given by a lognormal and a Gaussian distribution respectively with the forms

$$P_{st1}(x) = \frac{e^{-\frac{(\log[x] - \mu_1)^2}{2\sigma_1^2}}}{\sqrt{2\pi x \sigma_1}}$$

with mean $= e^{(\mu_1 + \frac{\sigma_1^2}{2})}$ and variance $= e^{(2\mu_1 + \sigma_1^2)} (e^{\sigma_1^2} - 1)$ and

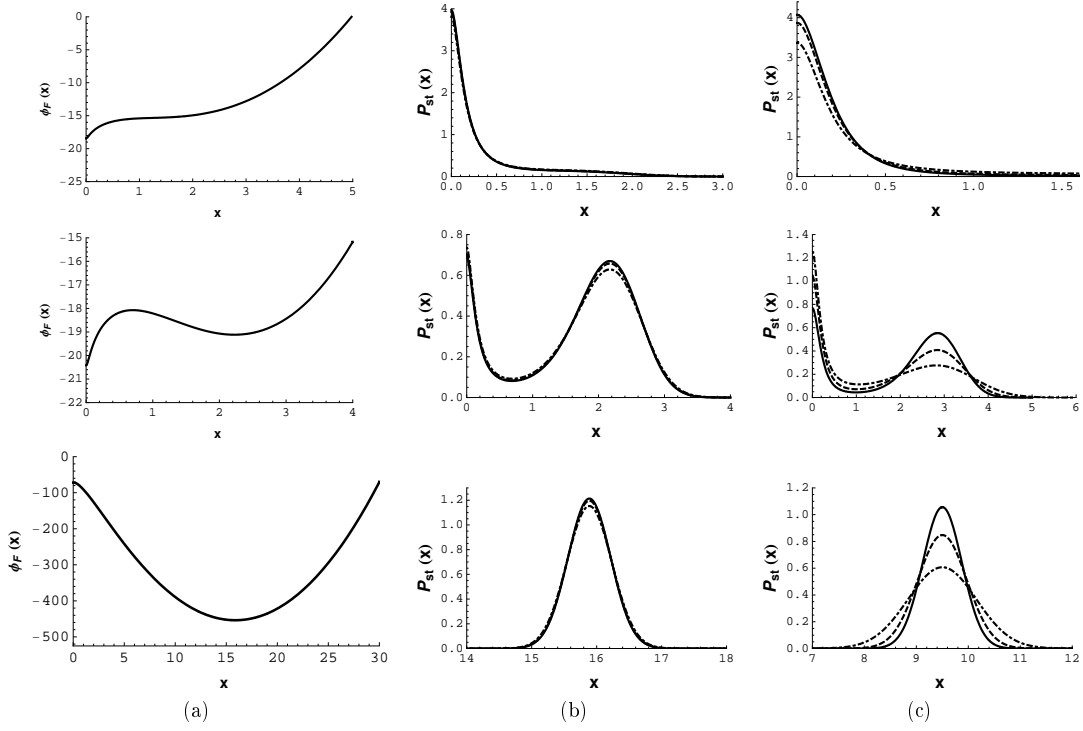


Figure 5. Both additive and multiplicative noise terms are present with the multiplicative noise associated with the nonlinear protein decay rate. Stochastic potential $\phi_F(x)$ (a) and the steady state probability distributions $P_{st}(x)$ ((b) and (c)) are displayed for $\alpha = 5.5, 5.96$ and 19 (b) and $\alpha = 14.8, 15.34$ and 21 (c). The other parameter values are fixed at $\delta = 0.01$, and $\phi = 20$ with $\gamma = 10$ (b) and $\gamma = 2$ (c). The noise strength D_2 is kept fixed at $D_2 = 0.1$ whereas the noise strength D_1 has the values $D_1 = 0.05$ (solid line), $D_1 = 0.4$ (dashed line), $D_1 = 1.2$ (dot-dashed line) in (b) and (c). The stochastic potentials in (a) are plotted for $D_1 = 0.05$ and $D_2 = 0.05$ with the other parameter values as in (b).

$$P_{st2}(x) = \frac{e^{-\frac{(x-\mu_2)^2}{2\sigma_2^2}}}{\sqrt{2\pi}\sigma_2}$$

with mean $= \mu_2$ and variance $= \sigma_2^2$.

The values of the parameters of the individual distributions as well as the coefficients a_1 and a_2 are listed in Fig. 4. The third panel in the figure shows the relative weight (in percentage) of the Subpopulation 2 as the additive noise D_2 is varied for the three different cases $\alpha = 5.8, 5.96$ and 6.1 . The lowest panel of Fig. 4 shows the variances of the probability distributions associated with the Subpopulation 2 versus D_2 in the three cases. The plots for Subpopulation 1 are similar in nature. Increased additive noise strength enhances noise-induced transitions over the potential barrier. For $\alpha = 5.8$, the transitions are from the low to the high expression state so that the relative weight of Subpopulation 2 increases with increased noise strength. In the other two cases, the relative weight of Subpopulation 2 decreases with the increase in the magnitude of D_2 . Increased additive noise strength further increases the spreading (measured by variance) of the protein distributions around the mean levels, i.e., brings in greater heterogeneity in the cell population. The lowest panel of Fig. 4 shows that the variance is not affected by α but depends only on the additive noise strength D_2 .

We next consider the case when both additive and multiplicative noise terms are present in the LE (Eq. (2)). We first assume that the multiplicative noise is associated with the maximum dilution rate ($\phi \rightarrow \phi + \epsilon(t)$), i.e., $g_1(x)$ in Eq. (2) is given by Eq. (6). We designate this type of noise as Type 1 multiplicative noise. Also, the two types of noise are taken to be uncorrelated, i.e., the parameter λ (Eq. (3)) is zero. Figure 5 shows the expression potential $\phi_F(x)$ (a) and the steady state probability distributions, $P_{st}(x)$ ((b) and (c)) versus x for $\alpha = 5.5, 5.96$ and 19 (b) and $\alpha = 14.8, 15.34$ and 21 (c). The other parameter values are fixed at $\delta = 0.01$ and $\phi = 20$ with $\gamma = 10$ (b) and $\gamma = 2$ (c). In computing $P_{st}(x)$, the additive noise strength D_2 is kept fixed at $D_2 = 0.1$ whereas the multiplicative noise strength D_1 has the values $D_1 = 0.05$ (solid line), 0.4 (dashed line) and 1.2 (dot-dashed line). The expression potentials in (a) are plotted for $D_1 = 0.05$ and $D_2 = 0.05$ with the other parameter values as in (b). The form of the stochastic potential is given by Eq. (14), which differs substantially from that of the deterministic potential. As in the case of Fig. 2, there is a progression from the monostable low expression state through a region of bistability to the monostable high expression state. From Fig. 5(b) one finds that the probability distributions $P_{st}(x)$ versus x are almost unaffected by changing the multiplicative noise strength D_1 from 0.05 to 1.2 . This is because $g_1(x)$, as given in Eq. (6), has a small value due to the high value of γ ($\gamma = 10$) in the denominator. Noticeable differences in the probability distributions appear (Fig. 5(c)) when γ has a lower value ($\gamma = 2$). One can conclude that increased fluctuations

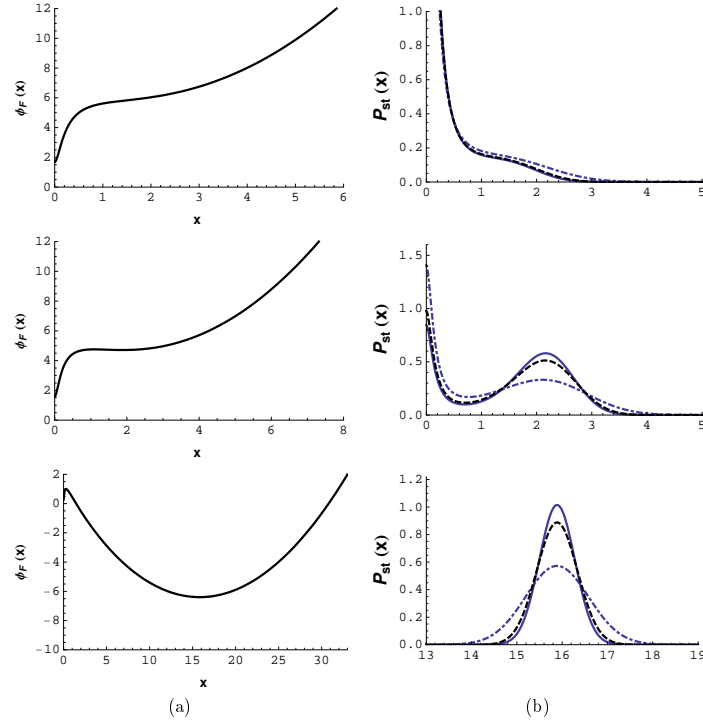


Figure 6. Both additive and multiplicative noise terms are present with the multiplicative noise associated with the effective rate constant for protein synthesis α . Stochastic potential $\phi_F(x)$ (a) and the steady state probability distribution $P_{st}(x)$ (b) are displayed for $\alpha = 5.5, 5.96$ and 19 . The other parameter values are fixed at $\gamma = 10$, $\delta = 0.01$, and $\phi = 20$. The noise strength D_2 is kept fixed at $D_2 = 0.1$ whereas the noise strength D_1 has values $D_1 = 0.05$ (solid line), $D_1 = 0.1$ (dashed line), $D_1 = 0.4$ (dot-dashed line) in (b).

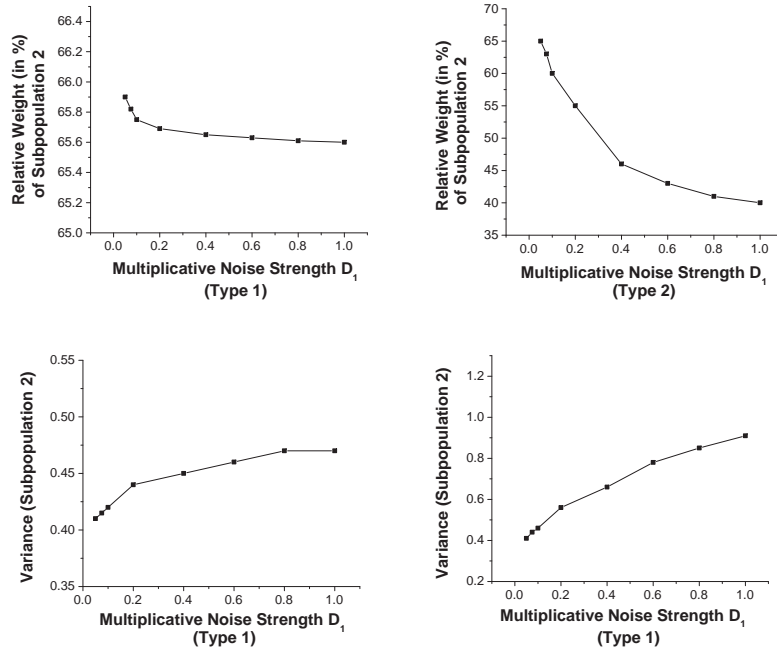


Figure 7. Relative weight of Subpopulation 2 and variance of the associated probability distribution as a function of Type 1 and Type 2 multiplicative noise strength D_1 , as computed using a mixture model. The additive noise strength is kept fixed at $D_2 = 0.1$. The value of $\alpha = 5.96$ with the other parameter values the same as in the case of Fig. 4.

in the maximum dilution rate parameter ϕ have little effect on $P_{st}(x)$ for moderately high values of γ . This is certainly not the case when $\gamma = 0$ or has lower values.

Figure 6 exhibits plots similar to Figs. 3 and 5 with the multiplicative noise term associated with the protein synthesis term, i.e., $g_1(x)$ is as given in Eq. (5). We designate this type of noise as Type 2 multiplicative noise. Increased multiplicative noise strengths now have a greater effect on the steady state probability distributions than in the earlier case when the multiplicative noise is associated with the maximum dilution rate ϕ (Fig.

5(b)). We again use the mixture model to determine the relative weights (in percentage) of the subpopulations as well as their variances as a function of the multiplicative noise strength D_1 with the noise being either of Type 1 (fluctuations in the maximum dilution rate ϕ) or Type 2 (fluctuations in the effective protein synthesis rate constant α). In both the cases, the additive noise strength is kept fixed at $D_2 = 0.1$. Figure 7 shows the plots of the relative weights of Subpopulation 2 and the variances of the associated probability distributions as a function of the multiplicative noise strength D_1 for both the Type 1 and Type 2 noises. The value of $\alpha = 5.96$ the deterministic potential of which is shown in Fig. 4. The other parameter values are kept the same as in the case of Fig. 3. In the case of the Type 1 noise, the relative weight of a subpopulation is very little affected by increased noise strength whereas the Type 2 noise has a substantially greater effect in bringing about phenotypic transitions between the stable expression states. For example, in the case of the Type 1 noise, the change in the relative weight is very small, from 18.1% to 18.4%, when D_1 is increased from 0.05 to 1.0. In the same range of values for D_1 , the change in the relative weight in the case of the Type 2 noise is much larger, from 22% to 47%. In the first case, the change in variance is also negligible, from ~ 0.45 to 0.51. In the latter case, the change in variance is more prominent, from ~ 0.45 to 0.95. Similar conclusions hold true for the other values of α considered in Fig. 4, namely, $\alpha = 5.8$ and $\alpha = 6.1$. Comparing Figs. 4 and 7, one finds that the additive noise has the more dominant effect in the spreading of the probability distributions. The emergent bistability model studied by us has the major feature that the protein decay rate is nonlinear in form. The significance of the results obtained by us is better understood if comparisons are made with the results obtained in the cases of unregulated gene expression and gene expression involving positive feedback (Hill coefficient $n > 1$) and linear protein dilution rate. The dynamics of protein concentration x in the case of unregulated gene expression is given by

$$\frac{dx}{dt} = k_x - \mu x \quad (17)$$

where k_x and μ denote the protein synthesis rate and the cell growth rate (rate of increase in cell volume) respectively. Experimental and theoretical results on the simple dynamical model indicate that multiplicative noise in the cell growth rate accounts for a considerable fraction of the total noise whereas the noise associated with the synthesis rate has only a moderate contribution [40]. In the case of cooperative regulation of gene expression involving a positive feedback loop but linear protein decay rate the dynamics of protein concentration is given by

$$\frac{dx}{dt} = \frac{\delta + \alpha x^n}{1 + x^n} - (\phi + 1)x \quad (18)$$

If the protein synthesis term is sufficiently nonlinear ($n > 1$), one can obtain bistability in specific parameter regions. The positive feedback amplifies the small fluctuations associated with the synthesis rate constant so that the contribution of the synthesis term to the total noise is not negligible compared to that of the protein decay term [30, 31]. In the case of emergent bistability, we have shown that for moderately large values of the metabolic cost parameter γ , the multiplicative noise associated with the maximum dilution rate parameter ϕ has little influence on the shape of the steady state probability distribution. In this case, the contribution of the protein synthesis term to the total noise is greater. The specific nonlinear form of the protein dilution rate appears to attenuate the effect of fluctuations in the maximum dilution rate parameter. For low values of the parameter γ , the effect of the multiplicative noise associated with the maximum dilution rate on the steady state probability distribution is noticeable but the extent of the region of bistability decreases as the γ values are lowered. In our study, the finding that the additive noise has the most dominant effect on the steady state protein distributions followed by the multiplicative Type 2 and Type 1 noise terms respectively is straightforward to explain. While the additive noise has a bare form, the noise in the effective synthesis rate constant α (Type 2 noise) is damped by a factor $\frac{x}{1+x} < 1$ and the noise in the maximum dilution rate ϕ (Type 1 noise) is damped even further by the factor $\frac{x}{1+\gamma x}$ for $\gamma > 1$.

We lastly consider the case when the additive and multiplicative types of noise are correlated, i.e., λ in Eq. (3) is $\neq 0$. Such correlations occur when the two types of noise have a common origin. We consider the multiplicative noise to be associated with the maximum dilution rate, i.e., $g_1(x)$ in Eq. (2) has the form shown in Eq. (6). Figure 8 shows the plots of the stochastic potential $\phi_F(x)$ (Eq. (14)) and the SSPD $P_{st}(x)$ (Eq. (12)) as functions of x . The noise strengths D_1 and D_2 are kept fixed at the values $D_1 = D_2 = 0.1$. The stochastic potential and $P_{st}(x)$ are shown for three values of λ , $\lambda = 0.7$ (dashed line), $\lambda = 0$ (solid line) and $\lambda = -0.7$ (dot-dashed line). The $\lambda = 0$ value is included for the sake of comparison between the correlated and uncorrelated cases. The parameter values are kept fixed at $\alpha = 15.34$, $\gamma = 2$, $\delta = 0.01$ and $\phi = 20$. We note from Fig. 8 that negative (positive) correlation decreases (increases) the depth of the right potential well. This is reflected in the steady state probability distribution with negative (positive) λ decreasing (increasing) the height of the second peak of $P_{st}(x)$ from that in the $\gamma = 0$ case. The changes in the depth of the left potential well and the height of the first peak of $P_{st}(x)$ are just the reverse since the probability distribution is

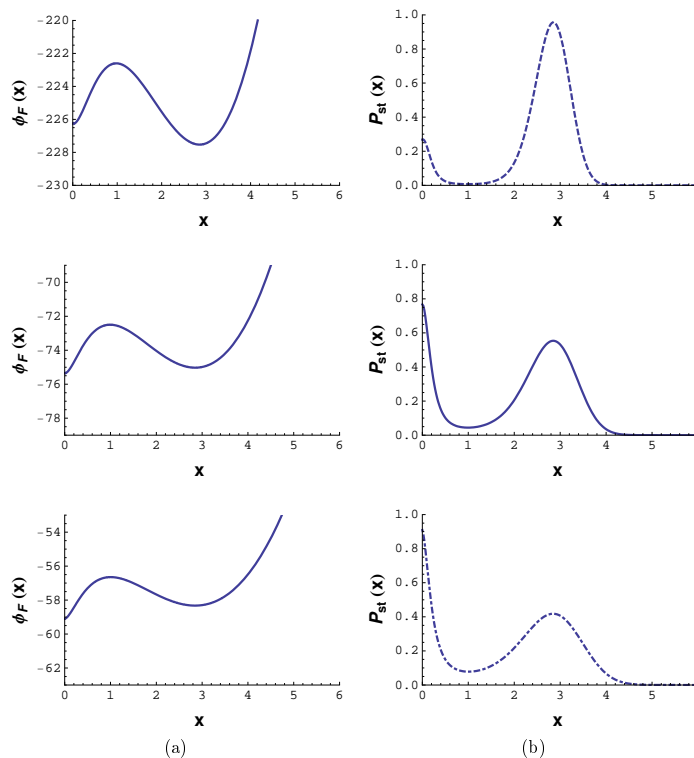


Figure 8. Both additive and multiplicative noise terms are present with the latter being associated with the maximum dilution rate parameter ϕ . The two types of noise are now correlated with λ being the strength of the correlation. Stochastic potential $\phi_F(x)$ (a) and the steady state probability distribution $P_{st}(x)$ (b) are displayed for $\alpha = 15.34$ where the system is bistable. The other parameter values are $\gamma = 2$, $\delta = 0.01$, and $\phi = 20$. The noise strengths are kept fixed at the values $D_1 = D_2 = 0.1$ and λ has the values $\lambda = 0.7$ (dashed line), 0.0 (solid line) and -0.7 (dot-dashed line) in the successive plots.

normalized.

IV. MEAN FIRST PASSAGE TIMES

We consider a bistable potential with two stable steady states at x_1 and x_2 ($x_1 < x_2$) separated by an unstable steady state at x_b defining the barrier state. In the presence of noise, exits from the potential wells are possible. The exit time is a random variable and is designated as the first passage time. In this section, we study the effects of additive and multiplicative noise on the mean first passage time (MFPT). Consider the state of the system to be defined by x at time $t = 0$ with x lying in the interval (a, b) . The first passage time $T(x; a, b)$ is the time of first exit of the interval (a, b) . The MFPT $T_1(x; a, b)$ is the average time of the first exit and satisfies the equation [28, 38, 39]

$$-1 = A(x) \frac{dT_1(x)}{dx} + \frac{1}{2} B(x) \frac{d^2 T_1(x)}{dx^2} \quad (19)$$

The MFPT $T_1(x_1)$ for exit from the basin of attraction of the stable steady state at x_1 satisfies Eq. (19) with the interval $(a, b) = (0, x_b)$ and boundary conditions given by

$$T_1'(a; a, b) = 0 \text{ and } T_1(b; a, b) = 0 \quad (20)$$

The prime denotes differentiation with respect to x , with reflecting boundary condition at a and absorbing boundary condition at b [28, 38]. In a similar manner, one can compute the MFPT $T_1(x_2)$ (from Eq. (19)) for exit from the basin of attraction of the stable state at x_2 . The interval is now $(a, b) = (x_b, \infty)$ with x_b and ∞ being an absorbing and a reflecting boundary point respectively, i.e.,

$$T_1(a; a, b) = 0 \text{ and } T_1'(b; a, b) = 0 \quad (21)$$

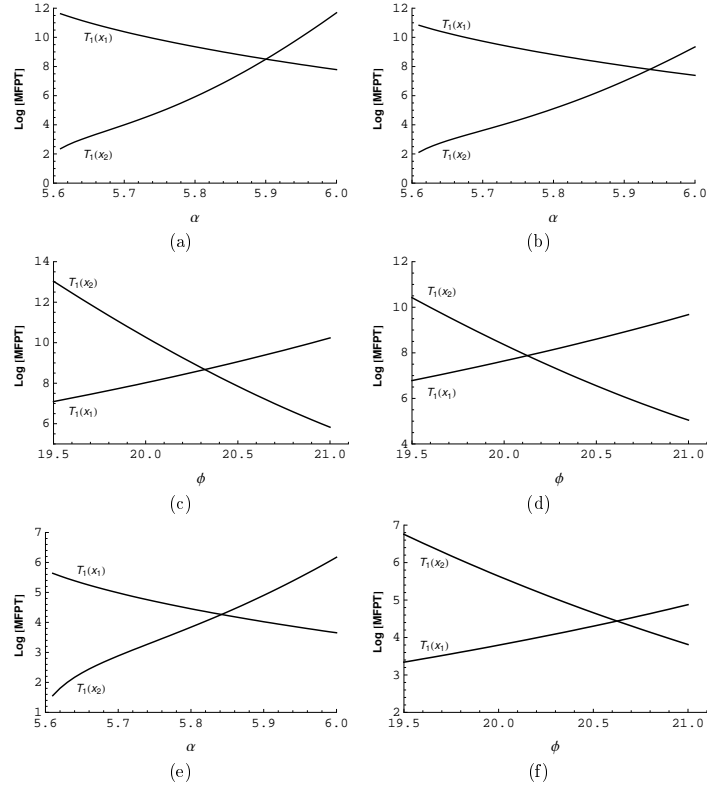


Figure 9. Plots of logarithm of MFPT versus α and ϕ . $T_1(x_1)$ and $T_1(x_2)$ are respectively the MFPTs for exits from the basins of attraction of the stable steady states at x_1 and x_2 . Six different cases are considered: (a) $\log [\text{MFPT}]$ versus α , with only the additive noise term (strength $D_2 = 0.05$) present, (b) $\log [\text{MFPT}]$ versus α with both additive and multiplicative (associated with the effective protein synthesis rate constant α) noise terms are present. The noise strengths are $D_2 = 0.05$ and $D_1 = 0.05$; (c) and (d) are similar respectively to (a) and (b) except that $\log [\text{MFPT}]$ is plotted as a function of ϕ ; (e) and (f) are similar respectively to (b) and (d) except that the additive noise strength is changed to $D_2 = 0.1$. In the cases (a), (b) and (e), $\phi = 20$. In the cases (c), (d) and (f), $\alpha = 5.96$. In all the cases the parameter $\delta = 0.01$ and $\gamma = 10$.

Figure 9 displays the results of the computations of the MFPTs in different cases: (a) the logarithm of the MFPT is plotted versus α with only the additive noise (strength $D_2 = 0.05$) present, (b) the same as in (a) but with the addition of the multiplicative noise associated with the effective protein synthesis rate constant α (the multiplicative noise strength $D_1 = 0.05$), (c) and (d) correspond respectively to the cases considered in (a) and (b) but now $\log[\text{MFPT}]$ is plotted as a function of the parameter ϕ (maximum dilution rate), cases (e) and (f) correspond respectively to (b) and (d) but with the additive noise strength changed from $D_2 = 0.05$ to $D_2 = 0.1$. In all the cases the parameter $\delta = 0.01$ and $\gamma = 10$. In the cases (a), (b) and (e), $\phi = 20$. In the cases (c), (d) and (f), $\alpha = 5.96$. Some features are worth pointing out in the plots of the MFPTs versus α and ϕ . The MFPT $T_1(x_1)$ decreases and $T_1(x_2)$ increases with increasing values of α (Figs. 9(a), 9(b) and 9(e)) whereas $T_1(x_1)$ increases and $T_1(x_2)$ decreases with increasing values of ϕ (Figs. 9(c), 9(d) and 9(f)).

In the $\log [\text{MFPT}]$ versus α plots the rise in $T_1(x_2)$ is sharper than that of $T_1(x_1)$ in the $\log [\text{MFPT}]$ versus ϕ plots. Similarly, in the first set of plots, the fall in $T_1(x_1)$ is slower than that of $T_1(x_2)$ in the second set of plots. Comparing the Figs. 9(b) and 9(e), the crossing point of the two MFPTs $T_1(x_1)$ and $T_1(x_2)$ shifts to the left when the noise strength is changed from $D_2 = 0.05$ (Fig. 9(b)) to $D_2 = 0.1$ (Fig. 9(e)). On the other hand, the crossing point shifts to the right in the $\log [\text{MFPT}]$ versus ϕ plots when the noise strength is increased (Figs. 9(d) and 9(f)).

A feature to emerge out of our study concerns the opposite effect that the two types of multiplicative noise have on the dynamics. This is more clearly seen in the plots of $\log [\text{MFPT}]$ versus α and ϕ in Fig. 9. The MFPT $T_1(x_1)$ decreases and $T_1(x_2)$ increases with increasing values of α whereas the opposite trend is observed for increasing values of ϕ . The shifts in the crossing points of the two MFPTs $T_1(x_1)$ and $T_1(x_2)$ when the additive noise strength is increased are in opposite directions in the two cases. Fig. 8 shows the effect of changing the correlation strength λ when the additive and multiplicative noise terms are correlated. The multiplicative noise appears in the maximum dilution rate parameter ϕ . Similar plots (not shown) are obtained when the multiplicative noise is associated with the effective protein synthesis rate constant. For this case as well as for the type of dynamics described by Eq. (18) (with the multiplicative noise associated with the protein synthesis rate constant), the effect of changing the strength of the correlation between the additive and multiplicative noises is opposite to that seen in Fig. 8.

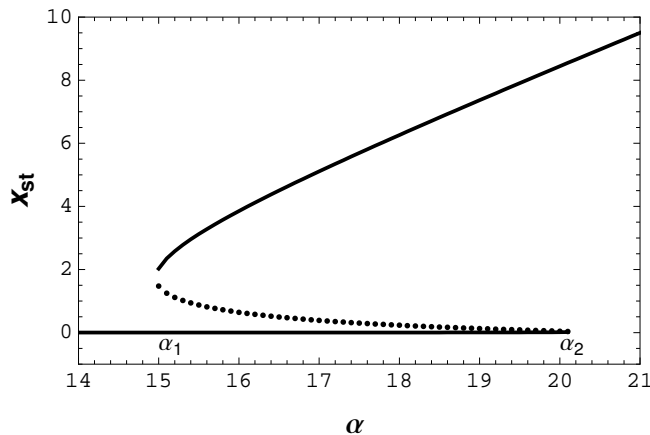


Figure 10. The steady state protein concentration x_{st} as a function of the parameter α exhibits hysteresis. The stable steady states are represented by solid lines whereas the dotted line describes the branch of unstable steady states. The bistable region separates the monostable low and high expression states. The points marked α_1 and α_2 denote the lower and upper bifurcation points.

Bistability is often accompanied by hysteresis [2, 4, 14] an example of which is shown in Fig. 10. In the figure, the steady state protein concentration x_{st} is plotted as a function of the parameter α . The solid branches represent the stable steady states separated by a branch of unstable steady states (dotted line). The bistable region separates the monostable low from the monostable high expression state. The transitions from the low to high and high to low expression states are discontinuous in nature and the special values of α (marked α_1 and α_2 in the figure) at which they occur are the bifurcation points of the dynamics. The path from the low to high expression state is not reversible. As α increases from low to high values, a discontinuous transition occurs at the upper bifurcation point α_2 . As α increases beyond this point, the steady state continues to be the high expression state. If one now reverses the direction of change in the value of α , i.e., decreases α from high to low values, there is no discontinuous transition at α_2 from the high to the low expression state. The reverse transition occurs only at the lower bifurcation point α_1 . The irreversibility of paths between the low and high expression states results in hysteresis. As pointed out earlier, in the case of the model under study, one can pass continuously from the low to the high expression state bypassing the region of bistability (Fig. 2(a)). An example of this type of behavior is obtained in the study on multistability in the lactose utilization network [8]. In the wild-type *lac* system, one cannot go from one region of monostability to the other without passing through a region of bistability. Appropriate modification of the natural system make it possible to connect the two regions of monostability via a path in which no discontinuities in the steady state expression levels occur. Fig. 11 exhibits the steady state probability distributions $P_{st}(x)$ versus x for different values of α when the path from the low to the high expression state is continuous (a) and when the transition path passes through a region of bistability (b). In the latter case, the probability distribution is bimodal in the intermediate range of α values. Only additive noise (strength $D_2 = 0.4$) is considered in both the cases and the other parameter values are $\delta = 0.01$ and $\gamma = 2$ with $\phi = 1$ in (a) and $\phi = 20$ in (b).

V. CONCLUSION

Emergent bistability is a recently discovered phenomenon [16] demonstrated in the case of a synthetic circuit. There is now some experimental evidence that a similar mechanism may be at work in microorganisms like mycobacteria subjected to nutrient depletion as a source of stress [12]. In emergent bistability, the coexistence of two stable gene expression states is an outcome of a nonlinear protein decay rate combined with a positive feedback in which cooperativity in the regulation of gene expression is not essential. The nonlinear protein decay rate is obtained if the synthesized proteins inhibit cell growth. Cell growth results in the dilution of protein concentration so that the protein decay rate is a sum of two terms: the dilution rate and the protein degradation rate. In most cases, the latter rate is sufficiently slow so that the protein decay rate is dominated by the dilution rate. In the case of emergent bistability, the dilution rate has the form $-\frac{\phi x}{1+\gamma x}$ where γ is the parameter representing the metabolic burden. For $\gamma = 0$, the dilution rate is linear in x as is the protein degradation rate. In this case, bistable gene expression via a positive feedback is possible only if the protein synthesis rate is sufficiently nonlinear. This is achieved when the regulatory proteins form multimers (dimers, tetramers etc.) so that x is replaced by x^n (n , the Hill coefficient, is > 1) in Eq. (1). This is the scenario that has been mostly studied so far whereas the issue of bistability due to a combination of non-cooperative positive feedback and nonlinear protein degradation rate is not fully explored.

In the case of bistable gene expression, the generation of phenotypic heterogeneity in a population of cells is

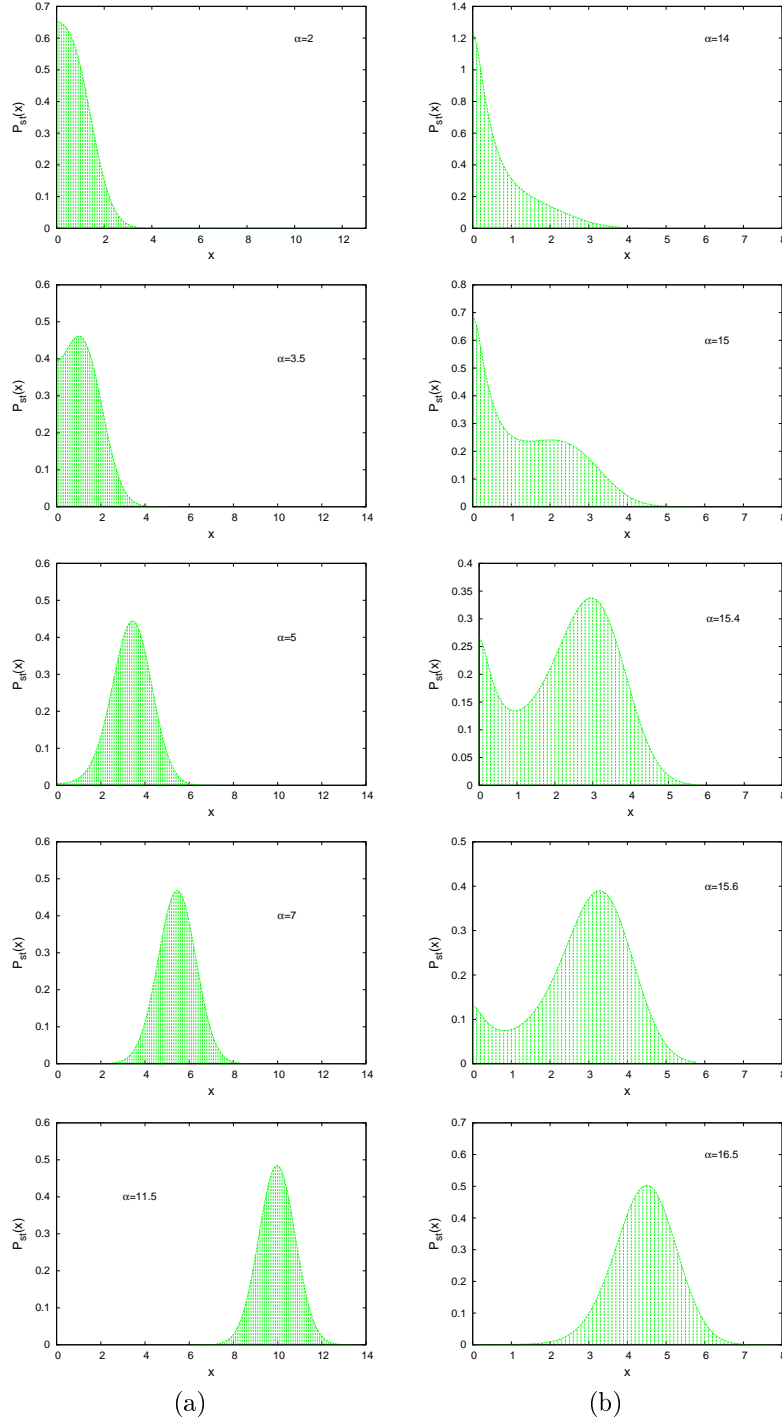


Figure 11. Steady state probability distribution $P_{st}(x)$ versus x . By changing the values of α , a transition from the low to the high expression state is obtained in a continuous manner (a) and by passing through a region of bistability (b). Only additive noise (strength $D_2 = 0.4$) is considered in both the cases and the other parameter values are $\delta = 0.01$ and $\gamma = 2$ with $\phi = 1$ in (a) and $\phi = 20$ in (b).

brought about by fluctuation-driven transitions between the stable expression states. In this paper, we analyze for the first time the effects of additive and multiplicative noise on the dynamics governing emergent bistability. Such studies acquire significance in the light of the fact that the generation of phenotypic heterogeneity enables a subset of a population of microorganisms to survive under stress. Examples of such stresses include depletion of nutrients, environmental fluctuations, lack of oxygen, application of antibiotic drugs etc. There is now considerable experimental evidence that positive feedback and gene expression noise provide the basis for the ‘advantageous’ heterogeneity observed in microbial populations [10, 24, 25]. The heterogeneity is usually in the form of two distinct subpopulations with low and high expression levels of a key regulatory protein, e.g., ComK in *B. Subtilis* [10, 25] and Rel in *M. Smegmatis* [11, 12]. High ComK levels in a fraction of the *B. Subtilis* population result in the development of ‘competence’ in the subset of cells enabling the subpopulation to adapt

to changed circumstances. The role of noise in bringing about phenotypic transitions from the low to high ComK expression states has been demonstrated experimentally [25], the reduction of noise results in a smaller fraction of cells in which competence is developed. In mycobacteria, high Rel levels in a subpopulation of cells (the so-called *persisters*) initiate the stringent response in these cells enabling the subpopulation to survive under stresses like nutrient depletion. The role of positive feedback and gene expression noise in the generation of two distinct subpopulations has been investigated experimentally in *M. Smegmatis* [11, 12]. As mentioned earlier, there is some experimental evidence [12] that the appearance of two distinct subpopulations, in terms of the Rel expression levels, is an outcome of emergent bistability. The key elements of the stringent response pathway and the ability to survive over long periods of time under stress are shared between the mycobacterial species *M. Smegmatis* and *M. Tuberculosis* [41–43]. The latter, the causative agent of tuberculosis, has remarkable resilience against various types of stress including that induced by drugs. A mechanism similar to that in *M. Smegmatis* may be responsible for the generation of the subpopulations of persisters (not killed by drugs) and non-persisters. Studies based on stochastic dynamic approaches provide knowledge of the key parameters controlling the operation of relevant gene circuits and the effects of fluctuations in these parameters towards the generation of phenotypic heterogeneity. The studies provide valuable inputs in the designing of effective strategies for drug treatment.

We have further pointed out the possibility of connecting the low and high expression states in a continuous manner. In this case, the region of bistability is bypassed so that no discontinuity in the steady state protein levels as seen in the hysteresis curve of Fig. 10 occurs. The bypassing is facilitated for low values of the ‘metabolic burden’ parameter α . Since experimental modulation of the parameter α and ϕ are possible [16], the theoretical prediction could be tested in an actual experiment. The dynamics considered in the present paper correspond to that of an average cell. In a microscopic model, the growth rates of the two subpopulations in the region of bistability could be different [16]. The potential impact of the growth rate on model parameters other than the protein dilution rate has been ignored in our study but this simplification is possibly well justified [18]. An issue that has not been explored in the present study is that of stochastic gene expression resulting in a bimodal distribution of protein levels in the steady state but without underlying bistability arising from deterministic dynamics. The issue of bimodality without bistability has been explored both theoretically [6, 39] and experimentally [44]. The present study is based on the approximate formalism involving the Langevin and FP equations. The chief advantage of the formalism lies in its simplicity and its ability to identify the separate effects of additive and multiplicative noises of various types. The formalism is valid when the number of molecules involved in the dynamics is large and the noise is small. Studies based on more rigorous approaches are desirable for a greater understanding of the effects of noise on emergent bistability.

ACKNOWLEDGMENT

SG acknowledges the support by CSIR, India, under Grant No. 09/015(0361)/2009-EMR-I.

-
- [1] B. Alberts, J. Lewis, A. Johnson, J. Lewis, M. Raff, K. Roberts, P. Walter, *Molecular Biology of the Cell*, Garland Science New York (2002)
 - [2] J. E. Ferrell Jr. , Curr. Opin. Cell Biol. 14, 140 (2002)
 - [3] J. R. Pomeroy, Curr. Opin. Biotechnol. 19, 381 (2008)
 - [4] W. K. Smits, O. P. Kuipers and J. -W. Veening, Nat. Rev. Microbiol. 4, 259 (2006)
 - [5] A. Y. Mitrophanov and E. A. Groisman, Bioessays 30, 542 (2008)
 - [6] R. Karmakar and I. Bose, Phys. Biol. 4, 29 (2007)
 - [7] F. J. Isaacs, J. Hasty, C. R. Cantor and J. J. Collins, Proc. Natl. Acad. Sci. USA 100, 7714 (2003)
 - [8] E. M. Ozbudak, M. Thattai, H. N. Lim, B. I. Shraiman, and A. van Oudenaarden, Nature 427, 737 (2004)
 - [9] J. J. Tyson , K. Chen and B. Novak , Nat. Rev. Mol. Cell. Biol. 2 908 (2001)
 - [10] J. -W. Veening, W. K. Smits and O. P. Kuipers, Annu. Rev. Microbiol. 62, 193 (2008)
 - [11] K. Sureka, B. Ghosh, A. Dasgupta, J. Basu, M. Kundu and I. Bose, PLOS One 3, e1771 (2008)
 - [12] S. Ghosh, K. Sureka, B. Ghosh, I. Bose, J. Basu and M. Kundu, BMC Syst. Biol. 5, 18 (2011)
 - [13] T. S. Gardner, C. R. Cantor and J. J. Collins, Nature 403, 339 (2000)
 - [14] C. M. Ajo-Franklin et al. , Genes Dev. 21, 2271 (2007)
 - [15] A. Becskei, B. Sraphin, and L. Serrano, EMBO J. 20, 2528 (2001)
 - [16] C. Tan, P. Marguet and L. You, Nat. Chem. Biol. 5, 842 (2009)
 - [17] J. Monod, Annu. Rev. Microbiol. 3, 371 (1949)
 - [18] S. Klumpp, Z. Zhang, T. Hwa, Cell 139, 1366 (2009)
 - [19] M. Krn, T. C. Elston, W. J. Blake, and J. J. Collins, Nature Rev. Genet. 6, 451 (2005)
 - [20] A. Raj and A. van Oudenaarden, Cell 135, 216 (2008)
 - [21] D. Fraser and M. Krn, Mol. Microbiol. 71, 1333 (2009)
 - [22] J. Hasty, J. Pradines, M. Dolink and J. J. Collins, Proc. Natl. Acad. Sci. USA 97, 2075 (2000)
 - [23] M. Acar, A. Becskei, and A. van Oudenaarden, Nature 435 (2005)

- [24] G. Balzsi, A. van Oudenaarden, and J. J. Collins Cell 144, 910 (2011)
- [25] H. Maamar, A. Raj and D. Dubnau, Science 317, 526 (2007)
- [26] M. Leisner, K. Stingl, E. Frey & B. Maier, Curr. Opin. Microbiol. 11, 553 (2008)
- [27] N. G. van Kampen, *Stochastic Processes in Physics and Chemistry* (North Holland, Amsterdam, 1992)
- [28] C. W. Gardiner, *Handbook of Stochastic Methods* (Springer-Verlag, Berlin, 1983)
- [29] D. T. Gillespie, Annu. Rev. Phys. Chem. 58, 35 (2007)
- [30] Q. Liu and Y. Jia, Phys. Rev. E 70, 041907 (2004)
- [31] Z. Cheng, F. Liu, X. P. Zhang, W. Wang. FEBS Lett. 582, 3776 (2008)
- [32] X. -D. Zheng, X. -Q. Yang and Y. Tao, , PLOS One 6, e17104 (2011)
- [33] H. Risken, *The Fokker-Planck Equation* (Springer-Verlag, Berlin, 1984)
- [34] W. Bialek, Adv. in Neural Information Processing 13, T. K. Leen, T. G. Dietterich and V. Tresp eds, pp 103 (MIT Press, Cambridge, 2001)
- [35] W. D. Jin, C. Li, and K. S. Zhi, Phys. Rev. E 50, 2496 (1994)
- [36] C. Li, W. D. Jin, and K. S. Zhi, Phys. Rev. E 52, 3228 (1995)
- [37] Y. Jia and J. -rong Li, Phys. Rev. E 53, 5764 (1996)
- [38] D. Gillespie, *Markov Processes: An Introduction for Physical Scientists* (Academic. Press, San Diego, CA, 1992)
- [39] T. B. Kepler and T. C. Elston, Biophysical Journal 81, 3116 (2001)
- [40] S. Tsuru, J. Ichinose, A. Kashiwagi, B. W. Ying, K. Kaneko, and T. Yomo, Phys. Biol. 6, 036015 (2009)
- [41] T. P. Primm, S. J. Andersen, V. Mizrahi, D. Avarbock, H. Rubin et al, J Bacteriol 182, 4889 (2000)
- [42] J. L. Dahl, C. N. Kraus, H. I. M. Bosh, B. Doan, K. Foley et al., Proc. Natl Acad. Sci. USA 100, 10026 (2003)
- [43] A. K. Ojha, T. K. Mukherjee and D. Chatterji, Infect. Immun. 68, 4084 (2000)
- [44] T. L. To, N. Maheshri, Science. 327(5969):1142 (2010)